Phenol Photodegradation on Platinized-TiO_2 Photocatalysts Related to Charge-Carrier Dynamics

Carina A. Emilio,[†] Marta I. Litter,[†] Marinus Kunst,[‡] Michel Bouchard,[§] and Christophe Colbeau-Justin*[,§]

Unidad de Actividad Química, Centro Atómico Constituyentes, Comisión Nacional de Energía Atómica, Avenida General Paz 1499, 1650 San Martín, Provincia de Buenos Aires, Argentina, Hahn-Meitner-Institut, Abteilung Solare Energetik, Glienicker Strasse 100, 14109 Berlin, Germany, Laboratoire d'Ingénierie des Matériaux et des Hautes Pressions (CNRS, UPR1311), Université Paris 13, 99 Avenue J.-B. Clément, Villetaneuse 93430, France

Received July 20, 2005. In Final Form: February 14, 2006

Three commercial TiO_2 compounds (Degussa P25, Sachtleben UV100, and Millenium PC50) and their platinized forms have been studied by the time-resolved microwave conductivity (TRMC) method to follow their charge-carrier dynamics and to relate it to the photocatalytic activity for phenol degradation in TiO_2 aqueous suspensions. The degradation reaction has been studied in detail, following the time evolution of the concentration of phenol and its intermediates by liquid chromatography. The results show that platinization has a distinct influence on the commercial compounds, decreasing globally the activity of P25 and increasing the activity of PC50 and UV100. An influence of charge-carrier lifetimes on the photoactivity of pure and platinized TiO_2 samples has been evidenced.

1. Introduction

Water decontamination is a very important subject of research in the field of the environmental chemistry. In this sense, semiconductor-based heterogeneous photocatalysis is a promising technology, very attractive for wastewater treatment and water potabilization. Since the first description of using titanium dioxide for water splitting after UV irradiation,[1] it has been shown that this activity can encompass a wide range of reactions, especially the oxidation of organic compounds. The study of the photodegradation of a large series of model substances has shown clearly that the majority of organic pollutants present in waters can be mineralized or at least partially destroyed.[2−5] The photocatalytic destruction or treatment of halogenated hydrocarbons, aromatics, nitrogenated heterocycles, hydrogen sulfide, surfactants and herbicides, and toxic metallic ions, among others, has been successfully achieved.[6−15]

Photocatalysis with semiconductors is the result of the interaction between charge carriers generated in the solid after light absorption and the surrounding medium. Thus, the charge carriers (electrons and holes) photogenerated in the solid, if they do not recombine, can participate in oxidation or reduction reactions leading to pollutant degradation. The most commonly used photocatalyst is titanium dioxide (TiO_2), which mainly crystallizes in two phases: anatase and rutile. Both phases absorb the near-UV light, and their band gaps are respectively 3.23 and 3.1 eV.[16] Although both crystallographic forms are photocatalytically active, anatase is known to be more active than rutile.[17]

Numerous works are devoted to the elaboration of highly active photocatalysts. The photocatalytic activity depends on the surface and bulk properties of the material,[16] thus leading researchers to attempt to enhance the activity by several ways: synthesis of TiO_2 powders by the classical sol−gel method,[18] the sol−gel method followed by freeze-drying[19] or by supercritical drying,[19−21] hydrothermal synthesis,[22] doping with transition metal ions,[23,24] and other different techniques.

From the early times of photocatalysis, metallization of a TiO_2 surface with Pt, Ag, Au, or other noble metals was proposed as a way to increase the photoactivity.[25] Since then, many papers have investigated the effect of metal incorporation,[26] particularly platinum, on various commercial titania for several degradation reactions. Among the most recent results, the following information can be extracted. Sun et al.[27] showed that platinization (1.0 and 1.5 wt % Pt loading) increases the activity of Hombikat UV100 (Sachtleben), but decreases the activity of P25 (Degussa)

* Corresponding author. Mailing address: Laboratoire d'Ingénierie des Matériaux et des Hautes Pressions, CNRS − UPR 1311, Université Paris 13, 99 avenue J.-B. Clément, 93430 Villetaneuse, France. Phone: +33 1 49 40 44 88. Fax: +33 1 49 40 34 14. E-mail: colbeau@limhp.univ-paris13.fr.

[†] Comisión Nacional de Energía Atómica.

[‡] Abteilung Solare Energetik.

[§] Université Paris 13.

(1) Fujishima, A.; Honda, K. *Nature* **1972**, *37*, 238−241.
(2) Turchi, G. S.; Ollis, D. F. *J. Catal.* **1990**, *122*, 178−192.
(3) Matthews, R. W. *Pure Appl. Chem.* **1992**, *64*, 1285−1290.
(4) Wold, A. *Chem. Mater.* **1993**, *5*, 280−283.
(5) Herrmann, J. M.; Guillard, C.; Pichat, P. *Catal. Today* **1993**, *17*, 7−20.
(6) Fox, M. A.; Dulay, M. T. *Chem. Rev.* **1993**, *93*, 341−357.
(7) Hoffmann, M. R.; Martin, S. T.; Choi, W.; Bahnemann, D. W. *Chem. Rev.* **1995**, *95*, 69−96.
(8) Hagfeldt, A.; Gratzel, M. *Chem. Rev.* **1995**, *95*, 49−68.
(9) Herrmann, J.-M. *Catal. Today* **1999**, *53*, 115−129.
(10) Pichat, P. *Water Sci. Technol.* **1997**, *35*, 73−78.
(11) Fujishima, A.; Rao, T. N.; Tryk, D. A. *J. Photochem. Photobiol., C* **2000**, *1*, 1−21.
(12) Howe, R. F. *Dev. Chem. Eng. Miner. Process.* **1998**, *6*, 55−84.
(13) Ollis, D. F. *CATTECH* **1998**, *2*, 149−157.
(14) Litter, M. I. *Appl. Catal., B* **1999**, *23*, 89−114.
(15) Bahnemann, D. *Sol. Energy* **2004**, *77*, 445−459.
(16) Linsebigler, A. L.; Lu, G.; Yates, J. T., Jr. *Chem. Rev.* **1995**, *95*, 735−758.
(17) Ohno, T.; Sarukawa, K.; Matsumura, M. *J. Phys. Chem. B* **2001**, *105*, 2417−2420.
(18) Piscopo, A.; Robert, D.; Weber, J. V. *J. Photochem. Photobiol., A* **2001**, *139*, 253−256.
(19) Dagan, G.; Tomkiewicz, M. *J. Phys. Chem.* **1993**, *97*, 12651−12654.
(20) Boujday, S.; Wunsch, F.; Portes, P.; Bocquet, J.-F.; Colbeau-Justin, C. *Sol. Energy Mater. Sol. Cells* **2004**, *83*, 421−433.
(21) Kolen'ko, Y. V.; Garshev, A. V.; Churagulov, B. R.; Boujday, S.; Portes, P.; Colbeau-Justin, C. *J. Photochem. Photobiol., A* **2005**, *172*, 19−26.
(22) Kolen'ko, Y. V.; Churagulov, B. R.; Kunst, M.; Mazerolles, L.; Colbeau-Justin, C. *Appl. Catal., B* **2004**, *54*, 51−58.
(23) Herrmann, J. M. *Catal. Today* **1995**, *24*, 157−164.
(24) Navio, J. A.; Testa, J. J.; Djedjeian, P.; Padron, J. R.; Rodriguez, D.; Litter, M. I. *Appl. Catal., A* **1999**, *178*, 191−203.
(25) Pichat, P.; Mozzanega, M. N.; Disdier, J.; Herrmann, J. M. *Nouv. J. Chim.* **1982**, *6*, 559−64.
(26) Subramanian, V.; Wolf, E. E.; Kamat, P. V. *J. Am. Chem. Soc.* **2004**, *126*, 4943−4950.
(27) Sun, B.; Vorontsov, A. V.; Smirniotis, P. G. *Langmuir* **2003**, *19*, 3151−3156.

10.1021/la051962s CCC: $33.50
Published on Web 03/18/2006

on phenol photodegradation. Sakthivel et al.[28] demonstrated that 0.8 wt % Pt loading increases the activity of P25 on Acid Green 16 photodegradation. According to Moonrisi et al.,[29] the presence of 1.0 mol % Pt on P25 enhanced the photodegradation rate of 4-chlorophenol (4-CP) under nitrogen bubbling, while it decreased the rate in the presence of dissolved oxygen.

Recently, some of us[30−32] studied the influence of UV100, P25, and TiONa PC50 (Millenium) platinization on structural parameters and on the degradation of various pollutants such as 4-CP, dichloroacetic acid (DCA), ethylenediaminetetraacetic acid (EDTA) and nitrilotriacetic acid (NTA). The results showed that platinization does not always enhance the activity, and that an optimum amount of platinum has to be found, with these features depending on the nature of both the pollutant and the photocatalyst.

The most prevalent explanation for the enhancement of the TiO_2 activity by platinum is the influence on charge-carrier separation. However, the previously mentioned works evidence that the influence of platinum is not clear and that the role of the $Pt-TiO_2$ interface needs further investigation. To try to understand the mechanisms taking place in the system, especially in the very beginning, and because of very fast processes, it is convenient to observe the charge-carrier dynamics using nanoscaled time-resolved techniques.

In this work, we chose a contactless transient photoconductivity method, time-resolved microwave conductivity (TRMC), as a tool for the investigation of the charge-carrier dynamics in TiO_2 materials. This technique has already proved to be very useful in pure and surface-treated TiO_2.[33−36] TRMC allows one to follow phenomena such as recombination, trapping, platinum, or interfacial charge transfer, occurring to UV-light-created charge carriers.

The charge-carrier dynamics observed by this method, coupled with structural results, is used to understand the activity of TiO_2 and $Pt-TiO_2$ in phenol photodegradation. Comparing short-time relaxation processes in solid after laser-pulsed strong photoexcitation with stationary processes during photochemical reaction may be daring, but Edge et al.[37] studied microwave photoconductivity on TiO_2 exposed to continuous polychromatic irradiation and showed that the mechanisms derived from this in a real-time method are consistent with those reported from TRMC measurements. Similarly, Bahnemann et al. pointed out that detailed kinetic analysis of time-resolved spectroscopic data reveals an extremely good correlation with independent adsorption measurements of model compounds on TiO_2.[38]

Additionally, TRMC has already been successfully used to correlate structural parameters, charge-carrier dynamics, and the photodegradation of phenol in TiO_2 systems.[20−22]

Platinized UV100, P25, and PC50 samples, synthesized previously by Emilio et al.,[32] were studied by TRMC and compared with pure samples to study the influence of platinization on the evolution of formation and the decay of charge carriers. In parallel, the activity of the photocatalysts for phenol photodegradation in water has been studied and correlated to charge-carrier dynamics. As phenol photocatalytic degradation mechanism have been established,[39] it has been chosen as a test reaction.

Table 1. Structural Data of TiO_2 Samples

sample	phase composition	crystallite size (nm)	S_{BET} ($m^2\ g^{-1}$)	pore diameter (Å)
P25	anatase 79% rutile 21%	22	51.0	315
1/P25	anatase 79% rutile 21%	24	48.5	300
PC50	anatase 100%	29	50.5	210
1/PC50	anatase 100%	22	44.2	248
UV100	anatase 100%	13	289.0	<50
1/UV100	anatase 100%	9	238.5	<50

2. Experimental Section

2.1. Photocatalysts Samples. Pure TiO_2 samples were commercial Degussa P25 (P25), Sachtleben Hombikat UV100 (UV100), and Millenium TiONa PC50 (PC50) powders, used as provided by the manufacturers. The platinized compounds were prepared by the impregnation of hexachloroplatinic(IV) acid hexahydrate on P25, UV100, and PC50, as described previously.[32] Photocatalysts with 1 wt % Pt loading were used in the present work and will be denoted as 1/P25, 1/PC50, and 1/UV100.

The structure and microstructure of platinized TiO_2 have also been previously studied by X-ray diffraction (XRD), scanning electron microscopy (SEM), and N_2 adsorption−desorption measurements.[32] In this work, the specific surface area and pore size distribution of PC50 and 1/PC50 were measured by the Brunauer−Emmett−Teller (BET) and Barrett−Joyner−Halenda (BJH) methods using nitrogen physisorption at 77 K (COULTER SA 3100).

Table 1 lists the structural and microstructural data of platinized and pure compounds.

2.2. Electronic Properties. The charge-carrier lifetimes in TiO_2 after UV illumination have been determined by microwave absorption experiments using the TRMC method.[40,41] TRMC measurements were carried out as previously described.[34] The incident microwaves were generated by a Gunn diode in the K_a band (28−38 GHz). The experiments were performed at 31.4 GHz, the frequency corresponding to the highest microwave power. The pulsed light source was a Nd:YAG laser providing an IR radiation at $\lambda = 1064$ nm. The full width at half-maximum of one pulse was 10 ns, and the repetition frequency of the pulses was 10 Hz. UV light (355 nm) was obtained by tripling the IR radiation. The light energy density received by the sample was 1.3 mJ cm^{-2}. At energy densities higher than 0.5 mJ cm^{-2}, such as those used in this work, it has to be taken into account that recombination phenomena during the pulse are important.[34]

A polymeric sample holder has been specifically designed for powder measurements.[34] With this design, the sample can be illuminated in the powder form, inside the waveguide. This allows the best microwave response.

2.3. Photocatalytic Tests. To test the photocatalytic behavior of the synthesized TiO_2 powders and the photodegradation of phenol in water, a well-known and established model reaction was chosen. The photocatalytic setup is displayed in Figure 1 and consisted of a cylindrical reservoir containing 400 mL of a catalyst suspension and the model compound, in which an ultraviolet mercury lamp (Cathodeon HPK 125 W) was dipped. This lamp contained a double-envelope glass used to circulate water for isolation and thermosta-

(28) Sakthivel, S.; Shankar, M. V.; Palanichamy, M.; Arabindoo, B.; Bahnemann, D. W.; Murugesan, V. *Water Res.* **2004**, *38*, 3001−3008.
(29) Moonsiri, M.; Rangsunvigit, P.; Chavadej, S.; Gulari, E. *Chem. Eng. J.* **2004**, *97*, 241−248.
(30) Hufschmidt, D.; Bahnemann, D.; Testa, J. J.; Emilio, C. A.; Litter, M. I. *J. Photochem. Photobiol., A* **2002**, *148*, 223−231.
(31) Siemon, U.; Bahnemann, D.; Testa, J. J.; Rodriguez, D.; Litter, M. I.; Bruno, N. *J. Photochem. Photobiol., A* **2002**, *148*, 247−255.
(32) Emilio, C. A.; Testa, J. J.; Hufschmidt, D.; Colon, G.; Navio, J. A.; Bahnemann, D. W.; Litter, M. I. *J. Ind. Eng. Chem.* **2004**, *10*, 129−138.
(33) Schindler, K.-M.; Kunst, M. *J. Phys. Chem.* **1990**, *94*, 8222−8226.
(34) Colbeau-Justin, C.; Kunst, M.; Huguenin, D. *J. Mater. Sci.* **2003**, *38*, 2429−2437.
(35) Martin, S. T.; Herrmann, H.; Choi, W.; Hoffmann, M. R. *J. Chem. Soc., Faraday Trans.* **1994**, *90*, 3315−3322.
(36) Martin, S. T.; Herrmann, H.; Hoffmann, M. R. *J. Chem. Soc., Faraday Trans.* **1994**, *90*, 3323−3330.
(37) Edge, M.; Janes, R.; Robinson, J.; Allen, N.; Thompson, F.; Warman, J. *J. Photochem. Photobiol., A* **1998**, *113*, 171−180.
(38) Bahnemann, D. W.; Hilgendorff, M.; Memming, R. *J. Phys. Chem. B* **1997**, *101*, 4265−4275.
(39) Sobczynski, A.; Duczmal, L.; Zmudzinski, W. *J. Mol. Catal., A* **2004**, *213*, 225−230.
(40) Kunst, M.; Beck, G. *J. Appl. Phys.* **1986**, *60*, 3558−3561.
(41) Warman, J. M.; De Haas, M. P. Puls Radiolysis. In *Puls Radiolysis*; CRC Press: New York, 1991; Chapter 6, p 101.

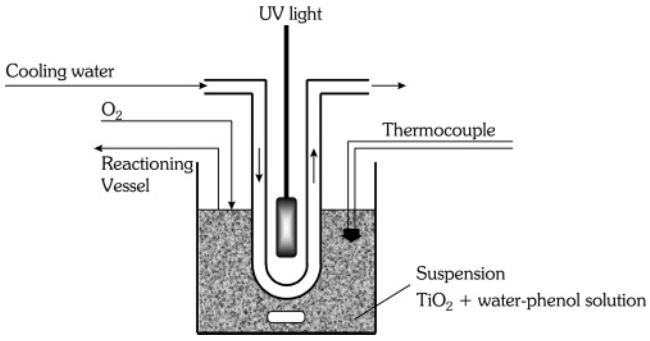

Figure 1. Experimental setup for the photocatalytic degradation of phenol over TiO_2 powder.

tization. It is a high-pressure mercury vapor arc lamp type, providing maximum energy at 365 nm, and the glass jacket prevents short UV light and IR radiation from entering the reservoir. The phenol was Aldrich 99% added at an initial concentration of 5.3×10^{-4} M (50 mg L^{-1}) in deionized water. The photocatalyst concentration was 1 g L^{-1}. The initial measured pH of the suspension was 6, and the pH was allowed to vary freely during the reaction. Before the reaction, the suspension was ultrasonicated for 30 min with stirring in the dark. During the reaction, the reservoir was magnetically stirred (900 rpm), and oxygen was continuously bubbled throughout the reaction time (20 mL/min). A photon flow per unit volume (P_0) of $(3.8 \pm 0.2) \times 10^{-5}$ einstein s^{-1} L^{-1} was determined by the ferrioxalate method,[42] using 400 mL of actinometric solution to keep the same conditions as those in the experiments. Samples (4 mL) were withdrawn every 10 min for an hour and two additional samples were taken at 75 and 90 min. After filtration through a 0.20-μm pore size poly(tetrafluoroethylene) (PTFE) membrane (TITAN), the solutions were analyzed by high-performance liquid chromatography (HPLC). Analyses were carried out by using a Varian Prostar 230 ternary gradient pump combined with a Prostar 330 photodiode array detector (D2 lamp) by a method developed in our laboratories. For elution, an isocratic mobile phase consisting in 90% of H_2O and 10% acetonitrile (ACN), at a 1 mL min^{-1} flow rate, was used, with 270-nm detection. The column was an Adsorbosphere C18 reverse phase column (5 μm, l: 150 mm, ID: 4.6 mm, Alltech) combined with an All-Guard cartridge system (7.5 × 4.6 mm, Alltech). For data acquisition, Star software was used.

3. Results

3.1. Principles of TRMC and Charge-Carrier Dynamics. The principles of TRMC and the experimental setup were widely described in a previous paper.[34] This technique is based on the measurement of the change in the microwave power reflected by a sample, $\Delta P(t)$, induced by its laser pulsed illumination. The relative difference $\Delta P(t)/P$ can be correlated, for small perturbations of conductivity, to the difference of conductivity, $\Delta\sigma(t)$, according to eq 1:[40]

$$\frac{\Delta P(t)}{P} = A\Delta\sigma(t) = Ae\sum_i \Delta n_i(t)\mu_i \qquad (1)$$

where $\Delta n_i(t)$ is the number of excess charge carriers i at time t, and μ_i is their mobility. The sensitivity factor A is independent of time, but depends on the setup features, the microwave frequency, and conductivity of the sample.

For n-type semiconductors, such as TiO_2, the TRMC signal can be attributed to electrons because their mobility is much larger than that of the hole.[43] For low-mobility semiconductors such as TiO_2 (10^{-4}–10^{-5} m^2 V^{-1} s^{-1}), the microwave absorbance is due to free mobile electrons in the conduction band and in shallow traps.[35,36]

Table 2. Electronic Properties of Titania Powders Measured by TRMC

sample	I_{max} (mV)	$\tau_{1/2}$ (ns)	$\tau_{1/4}$ (ns)	$\tau_{1/8}$ (ns)
P25	9.2	35	160	1500
1/P25	8.4	25	80	280
PC50	8.1	185	3500	>10000
1/PC50	5.3	105	8000	>10000
UV100	7.6	23	55	210
1/UV100	3.4	15	30	35

The understanding of the whole decay is not obvious because various processes are taking place simultaneously. In anatase, there is a competition between a fast recombination process and a trapping of part of the holes, which, as said, do not contribute to the TRMC signal. Thus, this trapping process reduces the number of holes available for recombination, thereby increasing the lifetime of electrons. The decay of the excess electrons can then be controlled by the relaxation (emission) time of the trapped holes or by their slow recombination with the trapped holes. According to experimental evidences using surface treatments, these traps are probably localized at the surface.[33,34]

Forty nanoseconds after the beginning of the pulse, it can be considered that no more direct influence of the pulse should be observed on the signal. Therefore, to clearly understand the phenomena taking place, the TRMC signal may be analyzed in two parts corresponding to different dominant processes. A short-time range decay (0 to about 40 ns after the beginning of the pulse) concerning fast processes that are mainly the recombination of charge carriers, and a long-time range decay (about 40−10 000 ns) that can be related to processes involving trapped species. In this part, the decay of the excess electrons is controlled by their slow recombination with trapped or relaxed holes.[34,35] The main data provided by TRMC are given by I_{max}, and $\tau_{1/2}$, $\tau_{1/4}$, and $\tau_{1/8}$. The parameter I_{max} is the maximum value of the TRMC signal, and reflects the number of excess charge carriers created by the UV pulse that can be detected by this technique. It must be noted that this information is weighted by the mobility of the charge carriers and by the influence of charge-carrier decay processes during the excitation. As the signal decay is not purely exponential, the general decay shape is characterized by several halftime lives linked to charge-carrier lifetimes. The parameters $\tau_{1/2}$, $\tau_{1/4}$, and $\tau_{1/8}$ are the times necessary to reduce I_{max} to $I_{max}/2$, $I_{max}/4$, and $I_{max}/8$, respectively.

I_{max}, $\tau_{1/2}$, $\tau_{1/4}$, and $\tau_{1/8}$ are presented in Table 2, and whole TRMC signals are displayed on Figures 2−4. Each figure shows signals of the pure commercial compound and of its platinized form.

The TRMC signals of the three pure compounds were different in intensity but mainly different in decay, as can be observed from the figures and data of Table 2. PC50 shows the slowest decay, followed by P25 and then UV100, which has a quite fast decay with a signal not far from the detection limit after 200 ns.

Concerning Pt influence, both the short-time and the long-time ranges have to be separately analyzed. In the short-time range, the same effect was observed for the three commercial powders: the I_{max} value was always lower for the platinized form than for the pure catalyst, decreasing 9% for P25, 35% for PC50, and 55% for UV100 (see Table 2). In addition, it can be seen that platinum accelerates the short-time decay in the three cases, in view of the fact that the $\tau_{1/2}$ values are always higher for the nonplatinized form.

In contrast to the fast processes, different behaviors for charge-carrier decay due to slow processes in the three commercial

(42) Hatchard, C. G.; Parker, C. A. *Proc. R. Soc. A* **1956**, *235*, 518.
(43) Fonash, S. J. *Solar Cell Device Physics*; Academic Press: New York/London, 1981.

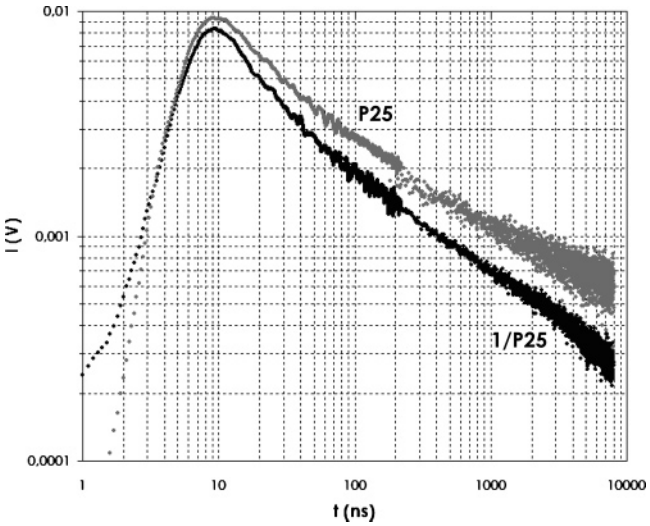

Figure 2. Influence of platinization on the P25 TRMC signal. Gray = P25, black = 1/P25.

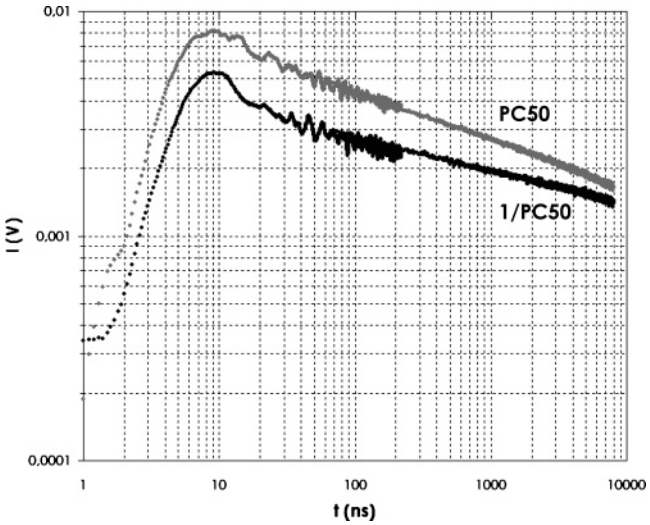

Figure 3. Influence of platinization on the PC50 TRMC signal. Gray = PC50, black = 1/PC50.

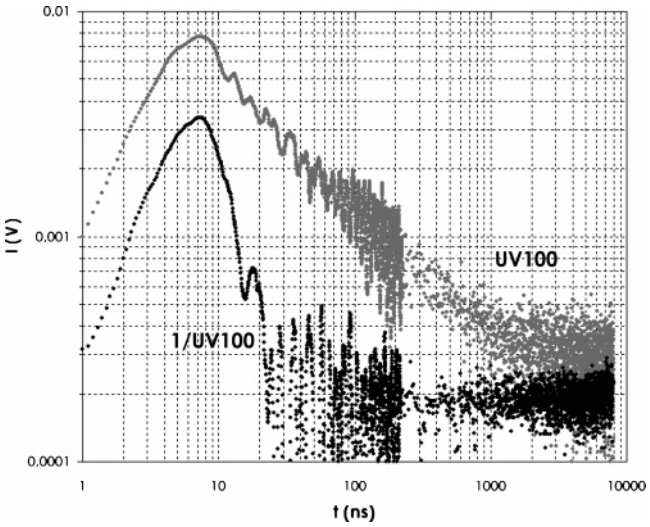

Figure 4. Influence of platinization on the UV100 TRMC signal. Gray = UV100, black = 1/UV100.

samples can be observed. In Figure 2, a similar long-time range decay behavior can be observed for both of the P25-based samples, but detailed $\tau_{1/2}$, $\tau_{1/4}$, and $\tau_{1/8}$ values (Table 2) show that the platinized form presents a faster decay, that is, charge carriers

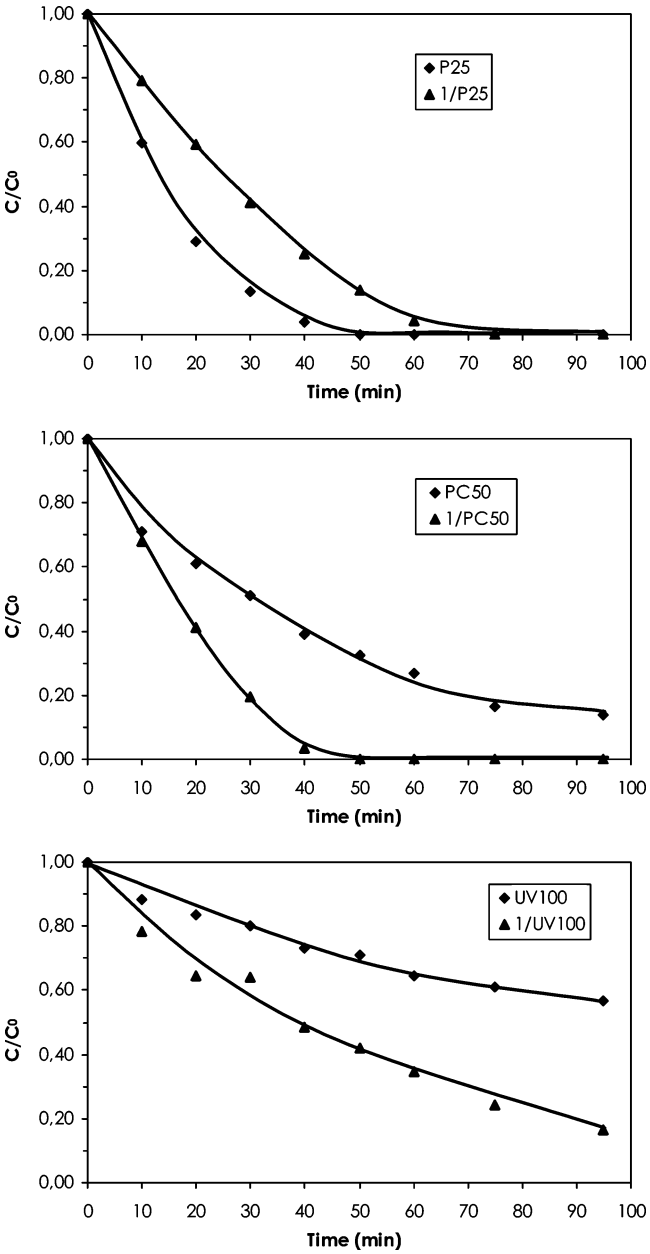

Figure 5. Disappearance of phenol over platinized TiO_2 catalysts in comparison to that over unmodified samples.

have a slightly shorter lifetime. Figure 3 shows the results of PC50 and 1/PC50. It can be observed that the long-range time decay is rather slow in the platinized form. This is also evidenced by the higher $\tau_{1/4}$ value of 1/PC50 depicted in Table 2. Concerning UV100, Table 2 and Figure 4 indicate that, although both UV100 forms present a fast decay in the long-time range, charge carriers in 1/UV100 decay much faster ($\tau_{1/8}$ is very close to $\tau_{1/4}$). Nevertheless, a residual constant signal is still detectable until 10 000 ns in both Hombikat samples (Figure 4).

3.2. Phenol Photodegradation. The phenol photodegradation results of pure and platinized TiO_2 are displayed in Figures 5 and 6, and in Tables 3 and 4.

Figure 5 displays the degradation profiles of normalized phenol concentration. These plots show, for all samples, an almost linear kinetic behavior at initial irradiation times, with a deceleration of the reaction at longer times. To characterize the kinetic behavior more properly, initial photonic efficiencies ζ_0 and degradation degrees at long irradiation times were considered. The initial rates and degradation extent after a 75-min irradiation were

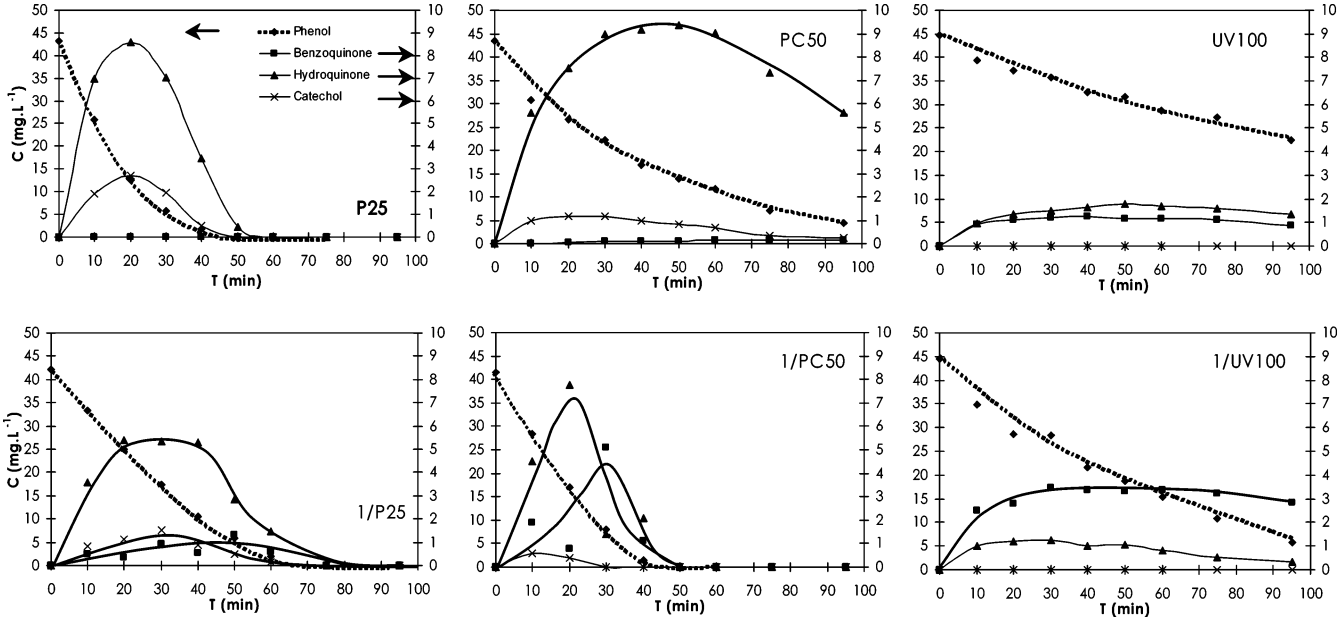

Figure 6. Evolution of intermediate compounds with platinized TiO_2 catalysts in comparison to that with unmodified samples.

Table 3. Initial Quantum Efficiencies and Extent of Phenol Degradation after 75-min Irradiation over TiO_2 Samples

sample	ζ_0 (%)	% degradation
P25	0.72	100
1/P25	0.45	100
PC50	0.41	84
1/PC50	0.64	100
UV100	0.17	39
1/UV100	0.33	76

Table 4. Amount of Intermediate Compounds after 50-min Illumination

sample	benzoquinone (mg L^{-1})	hydroquinone (mg L^{-1})	catechol (mg L^{-1})
P25	0.00	0.47	0.00
1/P25	1.32	2.86	0.51
PC50	0.12	9.35	0.83
1/PC50	0.00	0.00	0.00
UV100	1.16	1.80	0.00
1/UV100	3.34	1.06	0.00

extracted from the plots. ζ_0 is the ratio of the initial phenol photodegradation rate $(-dC/dt)_{t=0}$ and the incident light intensity.[44] Its validity for a proper comparison of photocatalytic systems has been experimentally verified.[45] ζ_0 was calculated according to

$$\zeta_0 = \frac{(-dC/dt)_{t=0}}{P_0} \qquad (2)$$

The results of ζ_0 and those corresponding to the degradation extent after a 75-min irradiation are presented in Table 3. As a general feature, it is worthwhile to mention that all the values of ζ_0 reported are quite low and comparable to values reported previously for 4-CP photodegradation under similar conditions.[30] These low values can be attributed to the weak adsorption of phenol (and 4-CP) onto the TiO_2 surface, in contrast with the higher results found in the photodegradation of stronger adsorbing compounds, such as EDTA and NTA.[32]

The main intermediate compounds in phenol or 4-CP photodegradation are hydroquinone, benzoquinone, and catechol.[27,39,46,47] Figure 6 displays the time evolution of the concentration of the initial compound and the three intermediates. In Table 4, the concentrations of the intermediates after 50 min of illumination time are presented. This time has been chosen because, after this period, phenol and all intermediate compounds are totally degraded when using P25.

Concerning the pure catalysts, all the results show differences between the photocatalytic behavior of the three samples, with P25 showing the highest efficiency, followed by PC50 and then by UV100, whose activity is really low. This order is the same as that found by Sun et al.[27] and by some of us for 4-CP, but it is not the same as that found with adsorbing compounds such as NTA (UV100 > PC50 > P25).[32] Figure 6 shows that benzoquinone is not observed over P25, while catechol is not detected over UV100.

It can be also observed that the effect of platinization depends mainly on the nature of the commercial powder. In the case of P25, all the parameters shown in Figure 5 and in Table 3 indicate a strong decrease in the activity of P25 after platinization: while 50 min are needed for total phenol degradation in the case of P25, the same reaction lasts 75 min over the platinized catalyst. This decrease is also observable in Figure 6 and Table 4. Phenol, as well as the intermediates are almost totally degraded after 50 min over P25, while they are still present after this time on 1/P25. These kinds of changes in the different ratios of intermediate compounds due to changing the nature of the photocatalyst have already been observed.[46] Sobczyñski et al.,[39] in their proposed mechanism of phenol photodegradation, point out that hydroquinone and *p*-benzoquinone reach an equilibrium, and that *p*-benzoquinone can be formed from hydroquinone in three different ways by attacking free •OH, surface trapped holes, or dissolved oxygen in water. As platinization influences the charge-carrier lifetimes, it could then influence the hydroquinone/*p*-benzoquinone equilibrium.

The effect of the PC50 platinization of PC50 is opposite that of P25 platinization. The parameters shown in Figure 5 and

(44) Serpone, N.; Terzian, R.; Lawless, D.; Kennepohl, P.; Sauve, G. *J. Photochem. Photobiol., A* **1993**, *73*, 11−16.
(45) Serpone, N.; Sauve, G.; Koch, R.; Tahiri, H.; Pichat, P.; Piccinini, P.; Pelizzetti, E.; Hidaka, H. *J. Photochem. Photobiol., A* **1996**, *94*, 191−203.
(46) Theurich, J.; Lindner, M.; Bahnemann, D. W. *Langmuir* **1996**, *12*, 6338−6376.
(47) Znaidi, L.; Seraphimova, R.; Bocquet, J. F.; Colbeau-Justin, C.; Pommier, C. *Mater. Res. Bull.* **2001**, *36*, 811−825.

Table 3 demonstrate a strong increase in the activity by platinization. In this case, at 50 min, phenol is almost completely degraded with the platinized PC50, while 30% of phenol is still present with the pure sample. The increase in the activity of the platinized sample is also evidenced by the evolution of the intermediates shown in Figure 6 and Table 4. In 50 min, the intermediates are completely degraded on 1/PC50, while, at the same time, an important amount of hydroquinone is still measured in the system with pure PC50. Platinization also leads to the appearance of a large amount of benzoquinone during the degradation, while the amount produced on the nonplatinized sample is very small. The effect of the platinization on UV100 is less obvious. ζ_0 and the degradation extent after 75 min (Table 3) show that 1/UV100 degrades phenol faster than does UV100. Nevertheless, in both cases, much more than 95 min will be needed to degrade phenol completely, as can be seen in Figure 5. On the other hand, a larger amount of benzoquinone is produced during the reaction over 1/UV100 than it is during that over UV100, and this intermediate is degraded at a lower rate in the platinized form (Figure 6).

4. Discussion

4.1. Pure Commercial Compounds. Comparison of the TRMC and phenol photodegradation results evidence that the activity cannot be directly related to charge-carrier dynamics. Many other structural and physical parameters are involved and have to be taken into account to properly understand the activity.

In previous works,[20−22] to correlate the structural, textural, and electronic properties of TiO_2 powders, the two linked parts of the photocatalytic mechanism have been considered separately. The first part, the *photo part*, concerns phenomena related to the interaction of the semiconducting material with light. This includes the absorption of photons and the creation, dynamics, and surface trapping of charge carriers. The second part, the *catalysis part*, concerns phenomena of the formation of radicals onto the surface and "surface reactivity", that is, the heterogeneous interaction between chemical species (H_2O, O_2, organic pollutants, etc.) and the oxide surface. For the photo part, results of TRMC measurements can be considered indicators of the interaction of the material with light. A high I_{max} value and a slow decay indicate a large amount of created charge carriers having long lifetimes and, thus, reveal a high crystalline quality. For the catalysis part, the specific surface area is the most relevant structural parameter because photocatalysis is an interfacial reaction: a higher specific surface area induces a higher number of accessible active sites and, consequently, a better reactivity.

This simple model helps one to understand the different activities observed on pure commercial powders. UV100 shows a high surface area (289 $m^2\ g^{-1}$), but the relatively low TRMC signal and lifetime ($I_{max} = 7.6$ mV, $\tau_{1/2} = 23$ ns) indicates a fast recombination rate resulting from the presence impurities, defects, or small crystal size, all of which lower the crystalline quality. These results are in accordance with the previous characterization results (XRD, SEM, and transmission electron microscopy (TEM) measurements).[32] The low number of available charge carriers then reduces the photoactivity. The initial quantum efficiency and global activity for phenol degradation are not very high (0.17 and 39% after 75 min, respectively; see Table 3), and this is in agreement with TRMC results.

Another commercial compound, TiO_2 Acros, pure anatase, which is not part of this work, was studied earlier by one of us,[47,48] presenting a quite opposite behavior. Its TRMC signal indicates a high crystalline quality ($I_{max} = 10$ mV, $\tau_{1/2} = 250$ ns), but its surface area is really low (7.7 $m^2\ g^{-1}$). Although phenol itself is quickly degraded over Acros in conditions similar to those of this paper (95% after 60 min of illumination),[47] its global activity is rather low because a large amount of intermediate compounds are formed. For example, 20 mg L^{-1} of benzoquinone and 8 mg L^{-1} of hydroquinone are produced after 50 min, and these intermediates are slowly degraded.

It is difficult to simultaneously control crystallinity and surface area during the synthesis, and most TiO_2 catalysts exhibit either a low crystallinity and a high surface area or the opposite.[30] Therefore, PC50 can be considered, from this point of view, as a good average compound: it does not possess the largest surface (50.5 $m^2\ g^{-1}$), and its TRMC features do not indicate the highest crystalline quality ($I_{max} = 8.1$ mV, $\tau_{1/2} = 185$ ns). A compromise of these conditions leads to a high photoactivity for phenol degradation (84% after 75 min, Table 3).

As P25 is not pure anatase but a mixture of rutile and anatase, it is difficult to consider this catalyst according to the above model.[22] The influence of the rutile phase in P25 has been previously studied, but some points remain unclear. The most common explanation is that one P25 particle is made of both phases.[49] Therefore, although rutile itself is a low active phase, the junction created by the two semiconductors helps the separation of the charge carriers because electrons migrate to the anatase phase and holes migrate to the surface. The rutile phase of P25 plays only the role of a charge separator and provides sites for oxidation.[27] The influence of rutile on photoactivity is obvious because, although P25 surface area is similar to that of PC50 ($\sim$50 $m^2\ g^{-1}$) and 5−6 times smaller than that of UV100, it presents the highest activity (100% of phenol degradation after 75 min of illumination) of the three pure commercial compounds compared here. Nevertheless, it must be noted that this effect of separation is not clearly evidenced by TRMC measurements, which show a rather fast decay ($I_{max} = 9.2$ mV, $\tau_{1/2} = 35$ ns). Some TRMC details have been mentioned by one of us in recent publications[47,48] and confirmed in this paper. As the measured signal of P25 is the result of the signals of the two phases, the rutile signal accelerates the decay of the global signal, because the TRMC signal of pure rutile is really different from the pure anatase signal for two reasons. First, the mobility of electrons in rutile is about 89 times lower than that in anatase,[27] which leads to a weaker signal intensity. Second, the lack of superficial hole traps in rutile leads to a shorter signal.[34] The effect of charge-carrier separation then might be hidden in P25.

4.2. Effect of Platinization. The results of structural and microstructural studies show that platinization does not influence the crystalline phase. It slightly reduces the surface area and modifies the pore diameter, but these small modifications are not large enough to influence the photoactivity in a significant way. Pt exerts a more important effect in the photo part than in the catalysis part.

As platinum similarly influences the three commercial powders in the short-time range of the TRMC decay, this influence can be commented globally. The decrease in I_{max} and $\tau_{1/2}$ by platinization can be interpreted according to three explanations. The first possibility is that the lower signal can be due to the creation of a smaller amount of charge carriers during the pulse. Platinum also absorbs photons[30,50] but these photons are not available for the creation of charge carriers in the semiconductor, and the metal would act as a shield for TiO_2. This hypothesis

(48) Chhor, K.; Bocquet, J. F.; Colbeau-Justin, C. *Mater. Chem. Phys.* **2004**, *86*, 123−131.

(49) Bickley, R. I.; Gonzalez-Carreno, T.; Lees, J. S.; Palmisano, L.; Tilley, R. J. D. *J. Solid State Chem.* **1991**, *92*, 178−190.

(50) Li, F. B.; Li, X. Z. *Chemosphere* **2002**, *48*, 1103−1111.

assumes first that Pt nanoparticles behave as a massive metal, and their contribution to the TRMC signal can be neglected, and second that superficial Pt does not drastically influence the electron bulk mobility. This effect would be more important on the intensity (I_{max}) than on the decay $\tau_{1/2}$ of the signal.

A second possibility would be that Pt acts as an impurity,[34] helping recombination processes during the pulse, and giving rise to faster recombination processes compared to those in the absence of the metal. This effect would decrease both I_{max} and $\tau_{1/2}$.

The third hypothesis would be that the electrons generated by the pulse are deeply trapped in platinum. As superficial platinum is an efficient site for O_2 reduction,[30,51] the electrons trapped in Pt are gaining efficiency for O_2 reduction, increasing the activity by accelerating the limiting step of the photocatalytic oxidation. Again, this hypothesis assumes that electrons in the nanosized platinum particles do not contribute to the TRMC signal. Pichat et al.,[52] in an early paper, analogously observed a decrease in the photoconductivity of platinized samples in comparison with pure TiO_2, due to the flow of electrons from the *n*-type semiconductor into the metal. A recent study of Subramanian et al.[26] using time-resolved absorption spectroscopy on Au/TiO_2 nanoparticles supports this last hypothesis. In this work, the authors measured the transient absorption decay at $\lambda = 675$ nm following UV pulse illumination ($\lambda = 308$ nm) because of electrons trapped by Ti^{4+}. A more intense signal was obtained for pure samples in comparison with that of Au-containing samples, and the lower intensity in this last case was interpreted as an indication of a fewer amount of electrons in the TiO_2 particles due to electrons lying in the Au-nanoparticles.

To summarize, in the short-time range, platinum acts as a shield, helps recombination, and activates trapped electrons. To relate these observations to photoactivity, it must be taken into account that these three phenomena occur simultaneously. The first two are detrimental for the activity (fewer charge carriers and higher recombination, respectively), while the third one would be favorable. Thus, the activity should be considered a result of these competing phenomena.

To understand the complete influence of platinum on commercial powders, it is also necessary to discuss the long-time range TRMC decay. As this influence is different for the three commercial powders, it will be discussed separately. Concerning P25, the results confirm those obtained by Schindler et al.[33] in the sense that platinization has a subtle effect, accelerating only very slightly the decay. The experimental data disagree with a prediction based on a model of a simple Schottky-type barrier between TiO_2 and Pt because, according to this model, due to a better separation of charge carriers, an increase in electron lifetimes would be expected. This can be interpreted as a lack of additional contribution of the superficial platinum to the separation, since, in P25, an anatase−rutile mixture, a sufficient separation already seems to be made by the junction between those two phases. Without a long-time range effect, the effects occurring in the short-time range seem to be dominant. The superficial platinum absorbs photons, helps recombination, and may activate a few electrons, but, in the short-time range, the predominant effect seems to be produced by the rutile phase. Pt cannot further increase the efficiency of charge separation in this TiO_2, whose two-phase composition already provides a very efficient suppression of recombination in liquid photocatalytic reactions. The effects negative to the activity are dominant, and platinization leads to a reduction of activity. Sun et al.[27] arrived at the same conclusion.

PC50 is a more simple system since it is purely anatase. Here, the experimental data seem to agree with the model of a simple Schottky-type barrier between TiO_2 and Pt. An increase in the lifetime of the electrons in the long-time range is observed, due, as expected, to a better separation of charge carriers caused by the barrier. This effect, in addition to the activation of electrons by platinum in the short-time range, seems to be dominant. The absorption of photons by platinum and fast recombination are then minor effects. The effects positive for photocatalysis are dominant here, with platinization increasing PC50 activity.

UV100 presents an intermediate behavior. It is also pure anatase, but, since the particles are small, surface phenomena are important. The experimental data disagree with a behavior due to a Schottky-type barrier. The decay is strongly accelerated by platinum, and this point is clearly negative for the activity. Thus, the only positive aspect that superficial Pt can cause to increase the activity is the activation of electrons, and this gives rise to a slight increase. This phenomenon may gain importance in UV100 because of the high surface area of the sample. The activation of electrons by platinization can help to degrade phenol faster. However, the deterioration of the long-time range signal is influential and may explain the difficulty of UV100 to degrade the formed benzoquinone. The lack of available charge carriers in the long-time range prevents the platinized compound from degrading the larger amount of benzoquinone created by the accelerated degradation of phenol.

It is worthwhile to note that the present TRMC results, related to the influence of platinization on photoactivity, only explain the results of degradation of nonadsorbing compounds such as phenol or 4-CP. Because the activity results are very different with adsorbing pollutants such as NTA or EDTA, TRMC experiments in the presence of these compounds should be made, which shall reveal the importance of the surface effects of the adsorbed compounds.

Vamathevan et al.[53] studied the influence of silverization on TiO_2−P25 on the photodegradation of various adsorbing or weakly adsorbing organic compounds such as phenol, salicylic acid, and sucrose. The effect on phenol photodegradation of P25 silverization is consistent with our results concerning P25 platinization. Furthermore, this work also shows that the metallization effect depends on the organic compound, and the authors propose completely different photodegradation mechanisms, depending on the adsorption of the organic species.

5. Conclusions

In the present work, three commercial TiO_2 compounds (P25, UV100, and PC50) and their platinized forms have been studied by the TRMC method to follow their charge-carrier lifetimes and to relate the results to the photocatalytic activity for phenol photodegradation.

The activity of pure photocatalysts has been explained in terms of surface area and charge-carrier lifetimes and compared with the platinized forms. The results show that platinization has a different influence, depending on the nature of the commercial forms. It decreases the activity of P25, while it increases the activity of PC50. The influence on UV100 is less obvious, and, with this catalyst, the activity is slightly increased by platinization. An influence of charge-carrier lifetimes on the photoactivity of platinized and pure TiO_2 samples has been evidenced. The

(51) Wang, C. M.; Heller, A.; Gerischer, H. *J. Am. Chem. Soc.* **1992**, *114*, 5230−5234.

(52) Disdier, J.; Herrmann, J.-M.; Pichat, P. *J. Chem. Soc., Faraday Trans. 1* **1983**, *79*, 651−660.

(53) Vamathevan, V.; Amal, R.; Beydoun, D.; Low, G.; McEvoy, S. *Chem. Eng. J.* **2004**, *98*, 127−139.

conclusions are that platinization has a distinct influence on charge-carrier lifetimes. On the three powders, in the short-time range of measurement, fewer charge carriers are created in the presence of Pt, which recombine faster, but some electrons may be activated by the metal. In the long-time range, platinization helps the separation of charge carriers in PC50 (as predicted by the effect of the formation of a Schottky-type barrier), has almost no effect on P25, and accelerates the decay of electrons in UV100. The observed activity is the result of the combination of the negative and positive effects of platinization. The activity of P25 seems to be determined by short-time range effects, while, in UV100 and mostly in PC50, the effects in the long-time range are the dominant ones.

Acknowledgment. This work was performed as part of the Comisión Nacional de Energía Atómica P5-PID-36-4 Program and the CNRS-LIMHP Program. C.A.E. thanks CNEA and CONICET for a doctoral fellowship. M.I.L. is a member of CONICET. M.B. thanks CNRS for a postdoctoral fellowship.

LA051962S